A PB-2 RITZ METHOD TO OBTAIN SEMI-ANALYTICAL BENCHMARK SOLUTIONS OF THICK PLATES IN BENDING

Tales de Vargas Lisbôa, taleslisboa@yahoo.com.br
Rogério José Marczak, rato@mecanica.ufrgs.br
Mechanical Engineering Department – UFRGS
Rua Sarmento Leite, 425 – Porto Alegre – RS – Brasil - 90050170

Abstract. *In this paper, the modified Rayleigh-Ritz method (pb-2) is applied to find the solution of moderately thick plates, under constant transverse load. Using the Mindlin plate formulation, a semi-analytical approximation is applied to generate displacement solutions for several types of boundary conditions. The influence of the shear strain in the displacement and resultant stresses is also investigated. A convergence study is presented to validate the results, which are discussed and compared with similar solutions from the literature.*

Keywords*: Ritz, moderately thick plates, semi-analytical solutions, benchmarking.*

1. INTRODUCTION

The increasing use of numerical tools to simulate the mechanical behavior of several structural classes has been bringing issues about the validity of the results. These tools are used to obtain the approximate solutions of the differential equations that govern the component behavior. However, numerical tools must be tested with analytical or semi-analytical solutions, regarding the governing equations. Yet, many tools recently implemented on commercial software are not satisfactorily tested, and the absence of analytical solutions for many cases leads the developers to test their models against other numerical solutions of overly simplified structural theories. Besides the importance of analytical or semi-analytical solutions in benchmarking, these solutions are a great aid for designers in obtaining quick solutions for practical problems, without the need of numerical modeling. In addition, benchmark solutions are frequently used to support regulatory councils in many engineering fields, reducing the conservatism in cases where there are no similar solutions.

The field of shear deformable plates still lacks analytical benchmark solutions for many cases of geometry, boundary conditions and loading. It is usual to find inconsistent relations between tri-dimensional elasticity solutions and plate theories, but it is important to mention that they are generally not directly comparable, since the differential equations that govern each other are different, and the boundary conditions are incompatible. Therefore, the study of semi-analytical and/or analytical solutions still find place as necessary tools for validating numerical models or to assist engineers in preliminary designs.

Many researchers have published solutions for thick plates. Salerno and Goldberg (1960) were among the first to obtain a solution for plates including the transverse shear strain. Using the Reissner theory, they derived analytic solutions for Lévy plates under constant transversal load. Using the finite difference method, Craig (1987) obtained numerical solutions for simply supported plates using the Reissner formulation. The author explored the case in which a concentrated load is applied on the center of the plate. Kant and Hinton (1983), using the Segmentation Method, obtained numerical solutions for Lévy plates with Mindlin formulation. Cooke and Levinson (1983) published a general solution for Lévy plates, considering the Mindlin plate theory, but a mistake when simplifying the system of equations, making their solution valid only for Navier plates. More recently, Lee et. al. (2001) obtained analytical solutions for Lévy plates, departing from relationships between the classic plate theory and the Mindlin plate theory. Their solutions were based on series expansion of hyperbolic functions. Therefore, due a characteristic of the Lévy solution and the nature of hyperbolic functions, these solutions didn't show full symmetry in cases with symmetric loads and boundary conditions. Following the same line of latter authors, Wang et. al. (2001) related the Mindlin plate theory with the Reissner plate theory. The authors presented analytic solutions for Reissner plates. Because of the same problems found in Lee et. al. (2001), again fully symmetric solutions have been not achieved.

The objective of the present work is to derive semi-analytical solutions for thick plates using the Mindlin (1951) plate model. The displacement field will be approximated by a linear combination of polynomial functions. The internal strain energy and the external work will be calculated through this displacement field. A modified Rayleigh-Ritz method (pb-2) will be applied to obtain stationary conditions and generate the final displacement field.

The modified Rayleigh-Ritz (RR) method, called pb-2, is based on a multiplicative decomposition of the approximation field, so that the approximation space not necessarily contains only cinematically admissible functions. The boundary conditions are imposed by multiplying the approximation function by a suitable set of functions. This modification greatly increases the versatility of the conventional method and, if used with computer algebra software, opens new possibilities for derivation of analytical solutions for many structural classes. The pb-2 method has been applied previously for a number of plate problems (static, dynamic, buckling, etc.). Kitipornchai et. al. (1994) applied the method to achieve dynamic solutions of trapezoidal plates under different boundary conditions. Wang and Aung (2007) used the method to obtain plastic buckling loads of thick plates. Wang et. al. (1997) used the method to obtain

resultant stresses on corner supported rectangular plates. Singh and Elaghabash (2003) use this methodology to get numerical solutions for large displacements of rectangular and rhombic thin plates.

2. MATHEMATICAL MODELING

The well known displacement field of Mindlin (1951) is described as:

$$U_\alpha(x_1, x_2, x_3) = -x_3\phi_\alpha(x_1, x_2), \qquad U_3(x_1, x_2, x_3) = u_3(x_1, x_2) \tag{1}$$

where U_α are the longitudinal displacements, U_3 the transverse displacement, u_α the membrane (in-plane) displacements, u_3 the transverse displacement, and ϕ_α the rotations along the coordinate axes. The coordinate x_3 is normal to the plate's middle surface. Herein, Greek indices vary from 1 to 2. Only transverse loadings are analyzed here, so the in-plane displacements will be not considered. Small displacements and isotropic linear constitutive behavior are also assumed throughout the text.

Using the displacement field of Eq.(1), the infinitesimal strain tensor for the plate deformation can be described as:

$$2E_{\alpha\beta} = -x_3(\phi_{\alpha,\beta} + \phi_{\beta,\alpha}), \qquad 2E_{\alpha 3} = u_{3,\alpha} - \phi_\alpha \tag{2}$$

where $E_{\alpha\beta}$ are the deformations on the plate middle surface and $E_{\alpha 3}$ are the transverse shear strains. Using the Hooke's law, the stress tensor are derived as functions of the displacement field:

$$\sigma_{\alpha\beta} = -x_3 G\left[\phi_{\alpha,\beta} + \phi_{\beta,\alpha} + \frac{\nu}{2(1-2\nu)}\phi_{\gamma,\gamma}\delta_{\alpha\beta}\right], \qquad \sigma_{\alpha 3} = \kappa^2 G(u_{3,\alpha} - \phi_\alpha) \tag{3}$$

where $\sigma_{\alpha\beta}$ are the stress on the plate middle surface and $\sigma_{\alpha 3}$ are the shear stresses. κ^2 is the conventional shear correction factor.

The resultant stresses are obtained through integration of the Cauchy tensor over the thickness, resulting:

$$\begin{aligned} &N_{\alpha\beta} = 0, \\ &M_{\alpha\beta} = -D(1-\nu)\left[\phi_{\alpha,\beta} + \phi_{\beta,\alpha} + \frac{\nu}{2(1-2\nu)}\phi_{\gamma,\gamma}\delta_{\alpha\beta}\right] \\ &Q_\alpha = \kappa^2 Gh(u_{3,\alpha} - \phi_\alpha) \end{aligned} \tag{4}$$

where $N_{\alpha\beta}$ are the normal ($\alpha = \beta$) and shear resultant stresses ($\alpha \neq \beta$) on the plate middle surface; $M_{\alpha\beta}$ are the bending ($\alpha = \beta$) and twisting ($\alpha \neq \beta$)moments; and Q_α are the transverse resultant stresses. The bending stiffness is given by $D = E_y h^3/12(1-\nu^2) = Gh^3/6(1-\nu)$, where E_y is the Young modulus. As expected, the normal and planar shear resultants on the plate middle surface are null due to the absence of membrane strains.

The conventional form of the RR method evaluates the weights of each function in the approximation function the minimization of the total energy functional:

$$\Pi = U - V_e$$

where U is the strain energy and V_e is the loading potential. The minimization of this functional reads:

$$\delta\Pi = \delta(U - V_e) = 0 \tag{5}$$

The interpolation of the displacements field considered in this work will be constructed in the following way:

$$u_3 \cong \hat{u}_3 = \mathbf{c}_3 g_3 \boldsymbol{\theta}_3, \qquad \phi_1 \cong \hat{\phi}_1 = \mathbf{c}_4 g_4 \boldsymbol{\theta}_4 \qquad \text{and} \qquad \phi_2 \cong \hat{\phi}_2 = \mathbf{c}_5 g_5 \boldsymbol{\theta}_5 \tag{6}$$

where $\mathbf{c}_3$, $\mathbf{c}_4$ and $\mathbf{c}_5$ are the constant sets for the displacement variables. The length of these vectors is nc, which is the number of functions in the interpolation. $\boldsymbol{\theta}_3, \boldsymbol{\theta}_4$ and $\boldsymbol{\theta}_5$ are the interpolation functions for each one of the interpolated variables. The functions g_3, g_4 and g_5 are such that:

$$g_i = \prod_{k=1}^{n} \left(x_j - x_{cc} \right)^{\delta_{cc}} \tag{7}$$

where $x_j - x_{cc}$ is the equation of the boundary lines of the plate. The exponent δ_{cc} can assume two values, associated to the type of boundary condition: 0 for free edges and 1 for fixed edges. In this case of the transverse displacement, the value 0 represents free edge and the value 1 represents a supported edge. On the rotational displacement, 0 represents free rotation and 1 represents fixed rotation in the edge. In supported edges, the transversal displacement receives δ_{cc} 1 and the rotation normal for this edge 0. In clamped edges, both values are 1. The sub-indexes i and j assume integer values, ranging from 3 to 5 and 1 to 2, respectively. Equation (7) is responsible for "stapling" the functions $\boldsymbol{\theta}_3$, $\boldsymbol{\theta}_4$ and $\boldsymbol{\theta}_5$ along the plate boundary, according to each boundary condition. Therefore Eqs.(6) automatically result in a set of cinematically admissible interpolation functions.

The first variation of the functional in Eq.(5) is now re-stated as:

$$\delta\Pi = \frac{\partial \Pi}{\partial \mathbf{c}_i} = \frac{\partial U_e}{\partial \mathbf{c}_i} - \frac{\partial W_e}{\partial \mathbf{c}_i} = 0 \tag{8}$$

As mentioned before, the interpolation space chosen is polynomial. This is due to the fact that Eqs.(7) is also polynomial, and therefore the integration of the functional E can be exactly accomplished by Gaussian quadrature.

The resulting product of the interpolation functions by the boundary condition functions is now mapped to a natural coordinate system. This mapping is identical to the well know finite element mapping used in isoparametric formulations. The new coordinate system is limited to [-1,+1].

The interpolation functions are built following the equation:

$$\boldsymbol{\theta}_{3m} = x_1^i x_2^{ng-i} \ , \ \boldsymbol{\theta}_{4m} = x_1^i x_2^{ng-i} \ \text{e} \ \boldsymbol{\theta}_{5m} = x_1^i x_2^{ng-i} \tag{9}$$

where n_g is the degree of the primary polynomial (the degree of the interpolation polynomial before the imposition of the boundary conditions), and

$$m = \frac{\left(n_g + 1\right)\left(n_g + 2\right)}{2} - i \tag{10}$$

Therefore, the final number of constants for each interpolation depends directly on the degree of the primary polynomial. The relation between the definitive number of constants and the degree of the primary polynomial is given by:

$$nc = \frac{\left(n_g + 1\right)\left(n_g + 2\right)}{2} \tag{11}$$

3. MATRIX FORMULATION

The application of the RR method demands the evaluation of the strain energy and the external work. The first one is evaluated by the integral of the internal product between the stress and strain tensors in the plate's volume. The second one is evaluated by the integral of the load times the lateral displacement over the area of the plate. Thus, the internal deformation energy is given by:

$$U_e = \frac{1}{2} \int_{\Omega} \mathbf{E}^T \mathbf{C} \mathbf{E} d\Omega \tag{12}$$

where:

$$\mathbf{E} = \left\{ -x_3 \phi_{1,1} \quad -x_3 \phi_{2,2} \quad -x_3 \left(\phi_{1,2} + \phi_{2,1} \right) \quad u_{3,1} - \phi_1 \quad u_{3,2} - \phi_2 \right\}^T \tag{13}$$

and

$$\mathbf{C} = G\begin{bmatrix} 2/1-\nu & 2\nu/1-\nu & 0 & 0 & 0 \\ 2\nu/1-\nu & 2/1-\nu & 0 & 0 & 0 \\ 0 & 0 & G & 0 & 0 \\ 0 & 0 & 0 & \kappa & 0 \\ 0 & 0 & 0 & 0 & \kappa \end{bmatrix} = G\mathbf{C}^{'} \tag{14}$$

The vector that groups the strains can be decomposed as:

$$\mathbf{E} = \mathbf{H}\boldsymbol{\varepsilon} \tag{15}$$

where:

$$\boldsymbol{\varepsilon} = \left\{\phi_{1,1} \quad \phi_{2,2} \quad \phi_{1,2} + \phi_{2,1} \quad u_{3,1} - \phi_1 \quad u_{3,2} - \phi_2\right\}^T \ ,$$

$$\mathbf{H} = \begin{bmatrix} -x_3 & 0 & 0 & 0 & 0 \\ 0 & -x_3 & 0 & 0 & 0 \\ 0 & 0 & -x_3 & 0 & 0 \\ 0 & 0 & 0 & 1 & 0 \\ 0 & 0 & 0 & 0 & 1 \end{bmatrix} \tag{16}$$

The vector in Eq. (16) can be written in terms of the displacement variables using a linear operator:

$$\boldsymbol{\varepsilon} = \mathbf{d}_{\mathbf{L}}\boldsymbol{\Delta} \tag{17}$$

with:

$$\mathbf{d}_{\mathbf{L}} = \begin{bmatrix} 0 & \partial\cdot/\partial x_1 & 0 \\ 0 & 0 & \partial\cdot/\partial x_2 \\ 0 & \partial\cdot/\partial x_2 & \partial\cdot/\partial x_1 \\ \partial\cdot/\partial x_1 & 1 & 0 \\ \partial\cdot/\partial x_2 & 0 & 1 \end{bmatrix},$$

and

$$\boldsymbol{\Delta} = \left\{u_3 \quad \phi_1 \quad \phi_2\right\}^T \tag{18}$$

Now the displacements interpolation of Eq. (6) can be written as functions of their corresponding constants, grouped in the following vector:

$$\boldsymbol{\lambda} = \left\{\mathbf{c}_3{}^T \quad \mathbf{c}_4{}^T \quad \mathbf{c}_5{}^T\right\}^T \tag{19}$$

so that the interpolated displacements are recovered through the following matrix multiplication:

$$\boldsymbol{\Delta} \cong \begin{Bmatrix} \hat{u}_3 \\ \hat{\phi}_1 \\ \hat{\phi}_2 \end{Bmatrix} = \begin{bmatrix} \boldsymbol{\psi}_3 & \mathbf{0} & \mathbf{0} \\ & \boldsymbol{\psi}_4 & \mathbf{0} \\ SIM & & \boldsymbol{\psi}_5 \end{bmatrix} \begin{Bmatrix} \mathbf{c}_3 \\ \mathbf{c}_4 \\ \mathbf{c}_5 \end{Bmatrix} = \mathbf{N}\boldsymbol{\lambda} \tag{20}$$

where the matrix $\mathbf{N}$ contains the cinematically admissible interpolation functions for each displacement.

After this modification, Eq.(12) can be rewritten as:

$$U_e = \frac{1}{2}\int_{\Omega} \boldsymbol{\lambda}^T \mathbf{N}^T \mathbf{d}_{\mathbf{L}}{}^T \mathbf{H}^T \mathbf{C}\mathbf{H}\mathbf{d}_{\mathbf{L}}\mathbf{N}\boldsymbol{\lambda} d\boldsymbol{\Omega} \tag{21}$$

While the loading potential is simply:

$$V_e = \int_\Lambda \mathbf{\Delta}^T \mathbf{P} d\Lambda = \boldsymbol{\lambda}^T \int_\Lambda \mathbf{N}^T \mathbf{P} d\Lambda \tag{22}$$

where $\mathbf{P} = \{q \quad m_1 \quad m_2\}$, and q is the transverse load, m_1 e m_2 are distributed moments applied on the plate's middle surface.

The first variation of the total potential in Eq. (8) now becomes:

$$\int_\Omega \left(\mathbf{N}^T \mathbf{d_L}^T \mathbf{H}^T \mathbf{C} \mathbf{H} \mathbf{d_L} \mathbf{N} d\Omega \right) \boldsymbol{\lambda} - \int_\Lambda \mathbf{N}^T \mathbf{P} d\Lambda = 0 \tag{23}$$

After the integrations are carried out, Eq.(23) generates a linear system of equations which can be solved for λ.

Before proceeding to the solution of Eq. (23), it is interesting to further reduce it. Observing that the matrices $\mathbf{N}$ and $\mathbf{d_L}$ are independent to x_3, the system of equations assume the form:

$$\int_\Lambda \left(\mathbf{B_L}^T \mathbf{R_L}^{'} \mathbf{B_L} d\Lambda \right) \boldsymbol{\lambda} = \frac{1}{G} \int_\Lambda \mathbf{N}^T \mathbf{P} d\Lambda \tag{24}$$

where:

$$\mathbf{B_L} = \mathbf{d_L} \mathbf{N}, \quad \mathbf{R_L} = \int_{-h/2}^{+h/2} \mathbf{H}^T \mathbf{C} \mathbf{H} dx_3 = G \begin{bmatrix} \frac{h^3}{6(1+\nu)} & \frac{\nu h^3}{6(1+\nu)} & 0 & 0 & 0 \\ \frac{\nu h^3}{6(1+\nu)} & \frac{h^3}{6(1+\nu)} & 0 & 0 & 0 \\ 0 & 0 & \frac{h^3}{12} & 0 & 0 \\ 0 & 0 & 0 & \kappa h & 0 \\ 0 & 0 & 0 & 0 & \kappa h \end{bmatrix} = G \mathbf{R_L}^{'} \tag{25}$$

The load can be parametrized as:

$$q_1 = q_0 a^4 / E_y h^4 \tag{26}$$

where q_0 is the actual load applied, q_1 is its normalized counterpart, a is a characteristic dimension of the plate (e.g. dimension of the plate side). This parameterization has been used by several authors (Lee et. al., 2001; Wang et. al., 2001), and adds numerical stability to the final system of equations.

Observing that the shear modulus divides the integral on the right side of Eq. (24), it suggests another parameterization:

$$q_2 = 2(1+\nu) q_1 = q_0 a^4 / G h^4 \tag{27}$$

Hence, the load vector $\mathbf{P}$, from Eq. (22), can be written as:

$$\mathbf{P} = \left\{ \frac{q_2 G h^4}{a^4} \quad 0 \quad 0 \right\}^T \quad \therefore \quad \mathbf{P} = \frac{q_2 G h^4}{a^4} \{1 \quad 0 \quad 0\} = \frac{q_2 G h^4}{a^4} \mathbf{P}^{'} \tag{28}$$

It is worth to note that the final result will not depend on the transverse Young modulus, when the loading is parametrizaded with this constitutive parameter. So, using the load parameter explicated in Eq. (27), the answer will depend the material compressibility, it is, the Poisson coefficient, only.

Finally, the solution of Eq. (24) is given as:

$$\boldsymbol{\lambda} = q_2 \eta^4 \left(\int_\Lambda \mathbf{B_L}^T \mathbf{R_L}^{'} \mathbf{B_L} d\Lambda \right)^{-1} \int_\Lambda \mathbf{N}^T \mathbf{P}^{'} d\Lambda \tag{29}$$

where $\eta = h/a$. Due the geometry parameterization, the upper and lower limits of the integrals are -1 and 1, respectively, for the two independent variables.

4. RESULTS

The formulation presented in sections 2 and 3 was implemented in a symbolic algebra software (Maple v.8) and tested for some well known benchmarks. Quadrilateral plates under four types of boundary conditions were analyzed under unitary transverse loading. The boundary conditions used are: all edges simply supported (SSSS), two opposite edges supported and the other two free (SFSF), two opposite edges simply supported and the other two clamped (SCSC), and all edges clamped (CCCC). The results obtained are normalized for easier verification against other references. The adopted normalizations are:

$$\overline{w}_1 = wD/q_0 a^4 \ , \ \overline{w}_2 = \overline{w}_1/\overline{w}_c \ , \ \overline{M}_{\alpha\beta} = M_{\alpha\beta}/q_0 a^2 \ , \ \overline{Q}_\alpha = Q_\alpha/q_0 a \tag{30}$$

where $\overline{w}_c$ is the convergence value found in the numerical analysis for each boundary and geometric conditions.

4.1 Convergence analysis

A convergence study was accomplished in order to estimate a value for n_g which could deliver accurate results for most cases. From this study it was found that SSSS, SFSF and SCSC plates needs only for odd values of n_g. Even values produced the same results than the odd one immediately below, for displacements and resultant stresses as well. In the case of CCCC plates, convergence was incremented only when increasing even n_g. Therefore only even numbers of terms were used for CCCC plates, and odd number of terms for the other boundary conditions.

Figure 1 shows the convergence behavior for square SSSS and CCCC plates. Note that convergence is not monotonic, but progressive with the increase of n_g. The maximum value tested was $n_g = 19$. For larger values the software used become unstable, but at that point the error was in the fourth significant digit of the normalized displacement. It was also found a visible influence of the plate thickness (*h*) on the convergence rate, particularly for lower values of n_g, as shown in Fig.1. Also, the larger the aspect ratio the greater the value of n_g necessary for convergence.

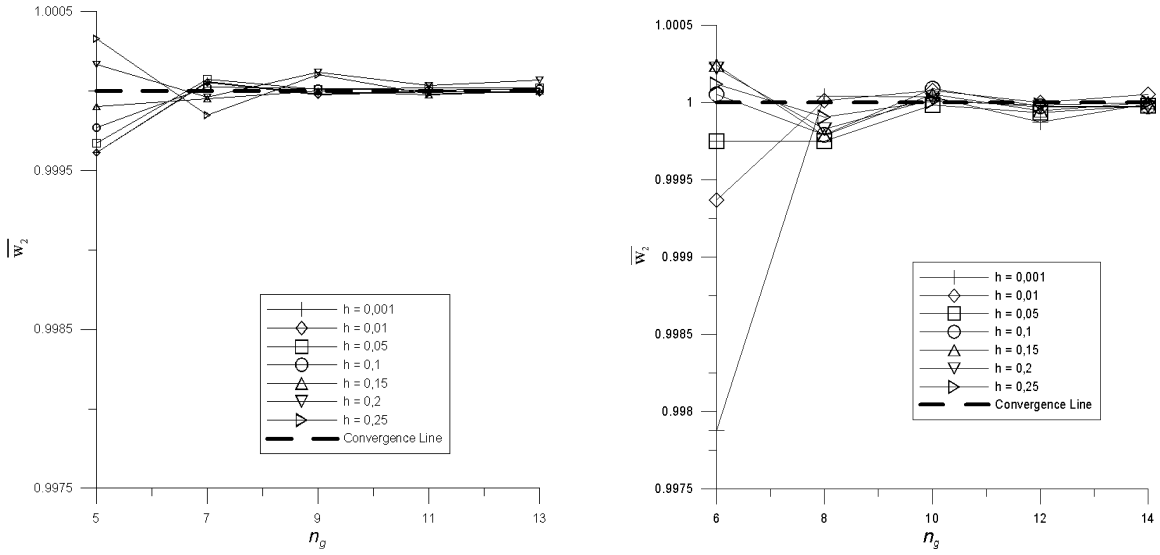

(a) (b)

Figure 1 - Convergence curves for square plates. (a) SSSS. (b) CCCC.

4.2 SSSS plates

Table 1 shows the center displacement values obtained for SSSS plates with different aspect ratios (*b*/*a*) using the proposed method. The results are compared with other solutions from the literature, and show very good agreement.

Although interpolation methods usually show a significant degradation of the stress values when compared to the displacement values, in the case of the SSSS plate the results for moments and shear stress resultants were also in good agreement with other solutions, as shown in Tab.2. Also worth to note in the results of Tabs.1-3 is the visible dependence of the plate thickness, differing from the classical plate theory (CPT) for larger values of *h*. Another interesting point to note is the clear lack of symmetry between Q_1 and Q_2 in all the solutions of Tab.3, not only in the classical results of Kant (1982), but also in the more recent works of Lee et. al. (2002) and Wang et. al. (2001). This is a

direct consequence of the non-symmetric series expansions used in those works, demanding a huge number of terms to achieve full symmetry for the stress resultants. The present results are perfectly symmetric.

Table 1 – $\overline{w}_1$ in the plate center SSSS (ν = 0.3 and n_g = 13)

h/a	$b/a=1$				$b/a=2$			$b/a=5$		
	Present work	Lee el al. (2002)	Salerno & Goldberg (1960)	Kant (1982)	Present work	Lee el al. (2002)	Salerno & Goldberg (1960)	Present work	Lee el al. (2002)	Salerno & Goldberg (1960)
0,001	0,0040624	-	-	-	0,010129	-	-	0,012971	-	-
0,010	0,0040645	0,00406	0,00406	0,00406	0,010132	0,01013	0,01013	0,012974	0,01297	0,01297
0,050	0,0041149	0,00411	0,00411	-	0,010210	0,01021	0,0102	0,013060	0,01306	0,01305
0,100	0,0042728	0,00427	0,00424	0,00424	0,010454	0,01045	0,01041	0,013328	0,01333	0,01327
0,150	0,0045360	0,00454	0,00446	-	0,010861	0,01086	0,01075	0,013774	0,01377	0,01365
0,200	0,0049040	0,00490	0,00478	0,00480	0,011430	0,01143	0,01123	0,014398	0,01440	0,01418
0,250	0,0053778	-	-	-	0,012162	-	-	0,015201	-	-

Table 2 – Stress resultants for square plates SSSS (ν = 0,3 e n_g = 13)

h/a	$M_{11}(s_1=0,s_2=0)$				$M_{22}(s_1=0,s_2=0)$				$M_{12}(s_1=0,s_2=0)$			
	Present work	Lee et. al. (2002)	Kant (1982)	Wang et. al. (2001)	Present work	Lee et. al. (2002)	Kant (1982)	Wang et. al. (2001)	Present work	Lee et. al. (2002)	Kant (1982)	Wang et. al. (2001)
CPT	0,0479				0,0479				0,0325			
0,001	0,0478	0,0479	-	0,0479	0,0478	0,0479	-	0,0479	0,0324	0,0325	-	0,0325
0,010	0,0478	0,0479	0,0478	0,0479	0,0478	0,0479	0,0479	0,0479	0,0324	0,0325	0,0324	0,0325
0,050	0,0478	0,0479	-	0,0480	0,0478	0,0479	-	0,0480	0,0324	0,0325	-	0,0322
0,100	0,0478	0,0479	0,0480	0,0482	0,0478	0,0479	0,0480	0,0482	0,0324	0,0325	0,0317	0,0316
0,150	0,0478	0,0479	-	0,0485	0,0478	0,0479	-	0,0485	0,0325	0,0325	-	0,0304
0,200	0,0478	0,0479	0,0484	0,0491	0,0478	0,0479	0,0485	0,0491	0,0324	0,0325	0,0299	0,0288
0,250	0,0478	-	-	-	0,0478	-	-	-	0,0324	-	-	-

h/a	$Q_1(s_1=-1,s_2=0)$				$Q_2(s_1=0,s_2=-1)$			
	Present work	Lee et. al. (2002)	Kant (1982)	Wang et. al. (2001)	Present work	Lee et. al. (2002)	Kant (1982)	Wang et. al. (2001)
CPT	0,333				0,333			
0,001	0,33	0,333	-	0,333	0,33	0,338	-	0,338
0,010	0,33	0,333	0,332	0,333	0,33	0,338	0,337	0,338
0,050	0,33	0,333	-	0,333	0,33	0,338	-	0,338
0,100	0,34	0,333	0,332	0,333	0,34	0,338	0,337	0,338
0,150	0,34	0,333	-	0,333	0,34	0,338	-	0,338
0,200	0,34	0,333	0,332	0,333	0,34	0,338	0,337	0,338
0,250	0,34	-	-	-	0,34	-	-	-

4.2 SCSC plates

A single case of SCSC plate was analyzed. The results for central displacement are shown in Tab.3, and compared with other available solutions. Once again, good agreement of the present results is observed.

Table 3 - $\overline{w}_1$ in plate center SCSC (ν = 0,3)

h/a	$b/a=1$				$b/a=2$			$b/a=5$		
	Present work	Lee el al. (2001)	Wang et. al. (2001)	Kant (1982)	Present work	Lee el al. (2001)	Wang et. al. (2001)	Present work	Lee el al. (2001)	Wang et. al. (2001)
0,001	0,0019172	-	-	-	0,0084451	-	-	0,012931	-	-
0,010	0,0019202	0,00192	0,00192	0,00192	0,0084492	0,00845	0,00845	0,012935	0,01293	0,01293
0,050	0,0019918	0,00199	0,00199	-	0,0085481	0,00855	0,00854	0,013021	0,01302	0,01311
0,100	0,0022087	0,00221	0,00220	0,00218	0,0088500	0,00885	0,00882	0,01329	0,01329	0,01338
0,150	0,0025558	0,00256	0,00254	-	0,0093379	0,00934	0,00926	0,01374	0,01374	0,01382
0,200	0,0030211	0,00302	0,00298	0,00293	0,010000	0,01000	0,00985	0,01436	0,01436	0,01445
0,250	0,0035957	-	-	-	0,010827	-	-	0,01517	-	-

4.3 CCCC plates

Analytical solutions for fully clamped plates are notably rarer than for other boundary conditions. The results obtained with the present method are compared with the excellent work of Taylor and Govindjee (2002) for thin plates in Tab.4. In order to achieve 10 digits accuracy, Taylor and Govindjee (2002) used a matrix system of 2000x2000. The values obtained by the methodology here presented were generated from a 315x315 system, using a polynomial of 13th degree. If the same system order could be used in the present method, the interpolation polynomial would be of degree 35, so that even more accurate results could be expected. Interestingly, the results for thin plates (h/a=0,001) point out for an error in the third digit of the classical solution of Timoshenko and Woinowski-Krieger (1959).

Table 4 - $\overline{w}_1$ in plate center CCCC (ν = 0,3)

h/a	$b/a = 1$		$b/a = 2$	
	Present work	Taylor & Govindjee (2002)	Present work	Taylor & Govindjee (2002)
0,001	0,0012654	0,001265319036	0,0025330	0,002532955769
0,010	0,0012678	-	0,002608	-
0,100	0,0015046	-	0,002962	-
0,250	0,0026580	-	0,004837	-

4.4 SFSF plates

Table 5 shows the displacement results in center of the plate and at the middle of the free edge for squared plates. Figure 2 illustrates the contour plot of the normalized lateral displacement (Fig.2a) and the normalized bending moment (Fig.2b) for a plate with b/a = 5. These results are ploted in the normalized space. This aspect ratio is used to make evident the characteristic anti-clastic curvature which appears in plates with this type of boundary conditions. . It can be noted that the methodology presented here captures the effect.

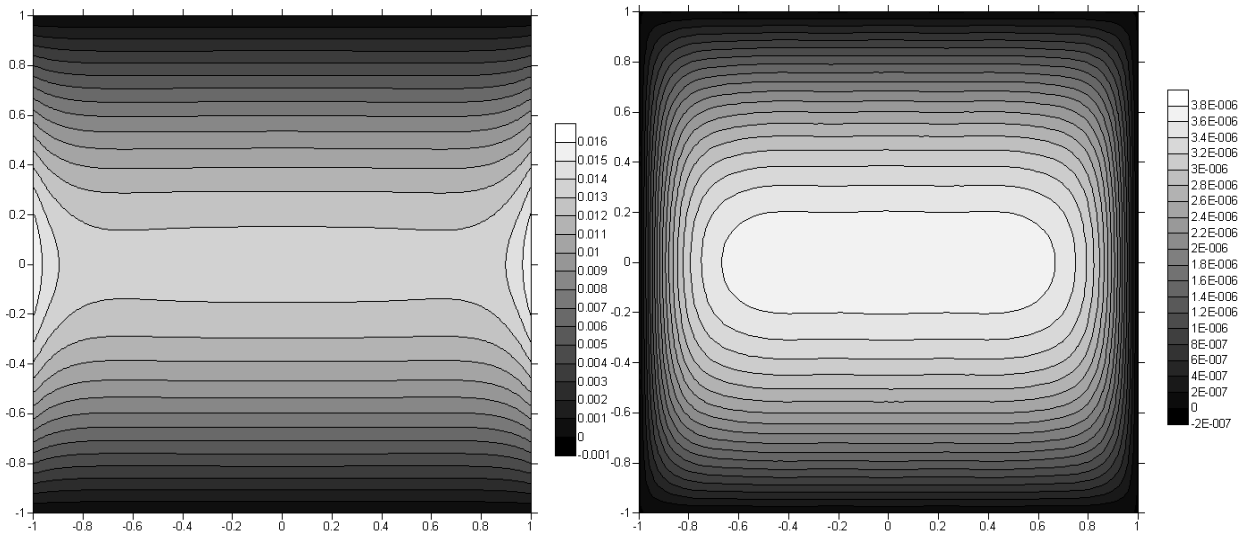

(a) (b)

Figure 2 - (a) $\overline{w}_1$ in center and (b) M_{11} in plates SFSF in normalized coordinates

Table 5 - $\overline{w}_1$ in plate center and $\overline{w}_1$ in free edge center in square plates SFSF (ν = 0,3)

h/a	Center of the plate				Middle of the free edge		
	Present work	Lee et. al. (2002)	Wang et. al. (2001)	Kant (1982)	Present work	Lee et. al. (2002)	Wang et. Al. (2001)
0,001	0,013094	-	-	-	0,015011	-	-
0,010	0,013097	-	-	0,0131	0,015023	-	-
0,050	0,013187	-	-	-	0,015214	-	-
0,100	0,013459	0,01346	0,01341	0,0134	0,015600	0,01560	0,01557
0,150	0,013910	0,01391	0,01379	-	0,016161	0,01616	0,01609
0,200	0,014539	0,01454	0,01433	0,0143	0,016898	0,01690	0,01678
0,250	0,015347	0,01536	0,01502	-	0,017809	0,01781	0,01762

4.5 Parametric solutions for benchmarking

A study on the influence of the plate thickness was carried out using the present implementation, in order to investigate the influence of the thickness over the results. This is not necessary in the CPT, since the thin plate equations are insensitive to the thickness. In thick plate analysis, on the other hand, the influence of the thickness is of the utmost importance, because it is the variable which controls the magnitude of the shear deformability. Due to the high memory requirements to deal with the symbolic expressions, the primary polynomial used for SSSS and CCCC in this case were of order 5 and 6, respectively, but, as show in Fig.1, the results still have at least 3 correct digits. These results are summarized in the plots of Fig.3, for SSSS and CCCC boundary conditions, respectively. By using the parametric form of the displacement, the agreement with other solutions is remarkable.

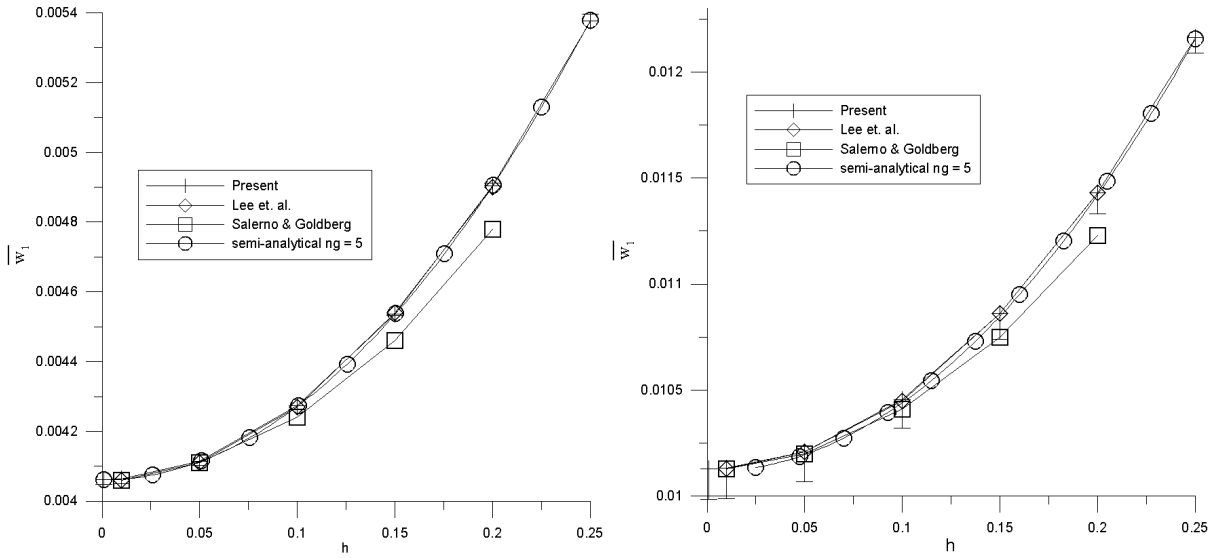

(a) (b)

Figure 3 - $\overline{w}_1$ in plates SSSS with (a) *b/a* = 1 and (b) *b/a* = 2

In order to retrieve a general solution of the center displacement as a function of the thickness, a curve fitting procedure was performed over the present results in Figs.3. The canonical form of the curve used is a third degree polynomial in *h*:

$$w_{center} = \frac{q_0 a^4}{D}\left(\alpha + \beta h + \gamma h^2 + \zeta h^3\right) \tag{31}$$

where the coefficients were adjusted for each type of boundary conditions and aspect ratio of the plate. Table 6 lists the coefficients obtained for two examples. One should note that in the limit $h \to 0$, Eq.(31) reduces to the thin plate solutions (Timoshenko & Woinowsky-Krieger, 1959)

Table 6 - Coefficients of the semi-analytical equation for $\overline{w}_1$ in the plate center.

SSSS	α	β	γ	ζ
b/a = 1	0,004061	0	0,0211	0
b/a = 2	0,01011	0	0,0326	0
CCCC	α	β	γ	ζ
b/a = 1	0,001262	0,00017	0,230964	-0,00584
b/a = 2	0,002496	0,000811	0,031346	0,004597

5. CONCLUSIONS

The *pb*-2 Rayleigh-Ritz method was developed and applied for the solution of rectangular shear deformable plates under transverse loading. Since the method enforces the boundary conditions through special functions which multiply the displacement interpolation functions, one can use general polynomial spaces to generate admissible solution spaces. Several cases of geometry and boundary conditions were analyzed, showing good agreement with reference solutions.

The method shows a fast convergence, and is particularly suitable for benchmarking purposes. Parametric solutions for rectangular plates were generated in semi-analytic form, including the influence of the thickness. The good performance of the proposed methodology encourages its extension to geometrically non-linear problems.

6. REFERENCES

Cooke, D. W., Levingson, M., 1983, "Thick rectangular plates – II. The generalised Lévy solution", International Journal of Mechanical Sciences, vol. 25, pp 207-215.

Craig, R. J., 1987, "Finite Difference Solutions of Reissner's Plate Equations", Journal of Engineering Mechanics, vol. 113, nº 1, pp 31-48.

Kant, T., 1982, "Numerical Analysis of Thick Plates", Computer Methods in Applied Mechanics and Engineering, vol. 31, pp 1-18.

Kant, T., Hinton, E., 1983, "Mindlin Plate Analisys by Segmentation Method", Journal of Engineering Mechanics, vol. 109, nº 2, pp. 537-556.

Kitipornchai, S.; Xiang, Y.; Liew, K. M.; Lim, M. K., 1994, "A Global Approach for Vibration of Thick Trapeziodal Plates", Computers and Structures, vol. 53, No. 1, pp. 83-92.

Lee, K. H., Lim, G. T., Wang, C. M., 2002, "Thick Lévy plates re-visited", International Journal of Solids and Structures, vol. 39, nº 1, pp. 127-144.

Mindlin, R. D., 1951, "Influence of Rotatory Inertia and Shear on Flexural Motions of Isotropic", Transation of ASME, Journal of Applied Mechanics, vol. 18, pp 31-38.

Salerno, V. L., Goldberg, M. A., 1960, "Effect of Shear Deformations on Bending of Rectangular Plates", Transation of ASME, Journal of Applied Mechanics, vol. 27, pp. 54-58.

Singh, A. V., Elaghabash, Y., 2003, "On finite displacement analysis of quadrangular plates", International Jornal of Non-Linear Mechanics, vol. 38, pp. 1149-1162.

Taylor, R. L., Govindjee, S., 2002, "Solution of clamped plate problems", Communications in numerical methods in Engineering, vol. 20, nº 10, pp. 757-765.

Timoshenko, S. P., Woinowski-Krieger, S., 1959, "Theory of Plates and Shells", McGraw-Hill Book Company, Auckland, 580 p.

Wang, C. M., Aung, T. M., 2007, "Plastic Buckling Analisys of thick plates using p-Ritz Method", International Journal of Solids and Strictures", vol. 44, pp 6239-6255.

Wang, C. M., Lim, G. T., Reddy, J. N., Lee, K. H., 2001, "Relationships between Bending Solutions of Reissner and Mindlin plate theories", Engineering Structures, vol. 23, pp 838-849.

Wang, C. M., Wang, Y. C., Reddy, J. N., 2002, "Problems and remedy for the Ritz method in determining stress resultants of corner supported rectangular plates", Computers and Structures, vol. 80, pp. 145-154.

7. RESPONSIBILITY NOTICE

The authors are the only responsible for the printed material included in this paper.